



Alla Fedorenko*, Evgen Kryuchkov,
Anna Voitsekhovska, Ihor Zhuk

Space Research Institute of the National Academy of Sciences of Ukraine
and State Space Agency of Ukraine, Kyiv, 03187, Ukraine

* Corresponding author: fedorenkoak@gmail.com

Study of the magnetic response to the AGW propagation based on measurements at the Akademik Vernadsky station

Abstract. To find the electromagnetic response to the propagation of atmospheric gravity waves (AGWs), wave fluctuations of the magnetic field were studied according to measurement data at the Ukrainian Antarctic Akademik Vernadsky station. We analysed continuous data for three components of the geomagnetic field of January–March 2024. We considered wave fluctuations of the magnetic field in the period range of 5–60 min, which correspond to medium-scale AGW in the atmosphere. From January–March, a total of 500 wave events were analysed. The amplitudes ranged from ~one nT to several tens of nT. Two dominant period groups were observed: ~5–12 minutes (including the Brunt–Väisälä period) and 25–30 minutes. We suppose that this pattern indicates a different origin of the AGW. This new result indicates the experimental possibility of separating the effects of AGW influences “from below” and “from above”. Time intervals during the day when magnetic field fluctuations are observed most often were determined. In all three magnetic field components, fluctuations are observed simultaneously in the evening. In geomagnetically quiet conditions, there is a daily asymmetry in the frequency of occurrence of meridional and zonal disturbances. Wave activity in the meridional B_x and vertical B_z components is registered mainly in the morning and evening. In the component B_y , wave disturbances prevail in the daytime from 10 to 14 hours (UT) and are also observed in the evening. In March 2024, there were two geomagnetic storms during which the amplitudes of magnetic field fluctuations increased simultaneously in different period ranges. The fluctuations may be caused by modulation of polar current systems and/or dynamo-current generation during the propagation of AGW at heights in the E-region of the ionosphere. Further studies are needed to establish which mechanism contributes more to the phenomenon.

Keywords: atmospheric gravity waves, geomagnetic pulsations, magnetic field fluctuations

1 Introduction

The atmosphere is a complex dynamic system that is always in motion under the effect of sunlight, solar wind, and the interplanetary magnetic field. These factors cause ionization of some parts of the atmosphere (the ionosphere) and the origin of electric fields and currents. Thus, waves propagating in the neutral atmosphere are reflected in

the fluctuations of the neutral parameters, the ionospheric plasma, and the electromagnetic component. This peculiarity of propagation complicates modelling wave processes in the atmosphere yet opens additional opportunities for their experimental diagnosing.

Studying the atmospheric gravity waves (AGWs) directly in the neutral upper atmosphere is severely limited by the lack of low-orbit satellites

equipped for these measurements (Innis & Conde, 2002; Fedorenko et al., 2015). The most common methods for studying the near space, including AGW spreading at the ionospheric heights, are ground-based diagnostics and magnetometry. Thus, wave activity in the atmosphere is studied mostly by observing travelling ionospheric disturbances (TIDs) (Negale et al., 2018; Zhang et al., 2019; Paznukhov et al., 2022). The influence of the electric and magnetic fields considerably complicates the interaction of neutral and ionized subsystems during the AGW propagation. In fact, the ionized component undergoes double control in the atmosphere. On the one hand, the ionospheric plasma and neutral particles are employed in all dynamic processes of the neutral atmosphere (winds, convection, tides, waves, etc.). On the other hand, plasma's behavior is largely controlled by electromagnetic processes in the atmosphere. As a result, the relationship between AGWs and TIDs varies at different heights depending on latitude and the changing geo- and heliophysical conditions.

The mechanisms behind the electromagnetic response to AGW propagation remain less understood compared to the well-documented AGW-TID interactions. The basics of electromagnetic disturbances' generation during AGW propagation at the ionospheric heights are presented in (Prakash & Pandey, 1985; Yampolsky et al., 2004; Lizunov et al., 2020). In the height range of 90–130 km, the ions follow neutral particles because of the collisions, yet the electrons are mostly controlled by the Earth's magnetic field. That is why, in the E-region of the ionosphere, all movements of the neutral particles displace the ions relative to the electrons, causing electric currents and fields (Jacobson & Bernhardt, 1985; Kelley, 1989). Yampolsky et al. (2004) analysed the electromagnetic effects of the AGW propagation at the E-region heights and estimated the respective amplitudes of the geomagnetic field's fluctuations. According to their conclusions, the main electromagnetic effects of AGW are (1) generation of the dynamo-current due to ions being captured by neutral particles; (2) periodical modulation of

the background currents flowing in the ionosphere because of conductivity changes following the changes in temperature, frequencies of the collisions and density of the charged particles in the AGW. Both effects lead to the geomagnetic field's fluctuations, which ground-based magnetometric measurements can register. According to the theoretical estimates (Yampolsky et al., 2004), the fluctuations' amplitudes are between single-digit nTs to dozens of nTs depending on the ionospheric conditions, AGW amplitudes, background currents, etc.

The effect of geomagnetic disturbances, dropout, magnetospheric-ionospheric currents, and other factors in space weather is the most noticeable in the polar areas. In the sunlit part of the polar cap, at the height of 90–130 km, there is formed in the ionosphere a two-vortex system of almost-horizontal currents perpendicular to the geomagnetic field's lines. The currents' magnetic effect can be registered on the ground (Kelley, 1989). Their configuration changes depending on the orientation of the interplanetary magnetic field (IMF), and the current grows significantly if the B_z component of this field is negative (for an example, see Fig. 6.28 in (Kelley, 1989)). Given powerful current systems in the polar areas, the contribution of the effect of current modulation by AGW outweighs the effect of dynamo-current generation. If the system of currents is restructured, the electromagnetic response in different magnetic field components will follow; a significant enhancement in the currents under geomagnetic activity will also increase the response to AGW.

Nowadays, magnetometry allows the registration of geomagnetic field fluctuations at different time scales with high accuracy. The measurement errors usually do not exceed 0.1 nT. Among the different types of geomagnetic field fluctuations, the most well-studied (in theory and practice) are the fluctuations with periods between some fractions of a second to several minutes (so-called geomagnetic pulsations). Processes in the magnetosphere and the solar wind generate a wide class of ultra-low-frequency (ULF) hydromagnetic waves,

observed as geomagnetic pulsations of various types. ULF waves originating in different areas of the magnetosphere have different frequencies and polarizations. They depend on the IMF orientation, solar wind conditions, and the magnetosphere (McPherron, 2005). The highest amplitudes are observed in the Pc5-type resonance magnetospheric pulsations in the auroral oval during a substorm's recovery phase (typical periods are from several minutes to 10 minutes) (Pulkkinen et al., 2003).

There have been much fewer studies of fluctuations with periods over 10 minutes (the upper bound for the Pc5 pulsations). Such fluctuations belong to the Pc6 and Ps6 types. Pc6 pulsations are an atypical kind of uninterrupted ULF pulsations as their periods are too long for resonance oscillations for a cavity in the magnetosphere regardless of its shape. These pulsations are linked with the magnetospheric tail dynamics (Heyns et al., 2020). Long-periodic, quasi-sinusoidal Ps6 pulsations are linked with magnetospheric substorms (Saito, 1978). They are mostly seen in the y-component of the magnetic field with periods of 5 to 40 min (Saito, 1978). This range, then, practically coincides with AGW periods. If long-periodic fluctuations are observed in geomagnetically quiet conditions, they can be manifestations of AGW propagation at the dynamo region heights.

Numerous ground-based and satellite observations confirm the permanent presence of AGWs/TIDs at different height levels of the polar atmosphere (Innis & Conde, 2002; Fedorenko et al., 2015; Negale et al., 2018; Zhang et al., 2019; Paznukhov et al., 2022). As AGWs propagate at the dynamo region heights, geomagnetic field fluctuations should be excited by generating dynamo current and (or) modulating the background currents. The purpose of the article is to study the electromagnetic response to AGW propagation in polar areas. We shall study the geomagnetic field's fluctuations with periods of 5 min to 1 hour using the data of a three-component magnetometer at the Akademik Vernadsky station. The periods correspond to middle-scale AGWs propagat-

ing through the atmosphere from various sources. The electromagnetic response to AGW propagation should also be observable in this period range.

In Section 2, we describe the methods of processing the measurement data. The behavior of the amplitudes of magnetic field fluctuations, daily patterns and distribution of fluctuations by periods are presented in Section 3. In Section 4, we discuss two possible mechanisms of the magnetic response of the AGW. Our conclusions are presented in Section 5.

2 Data and methods

The data for the study included the measurements of the geomagnetic field at the magnetic observatory of the Ukrainian Antarctic Akademik Vernadsky station (65°16'S, 64°15'W). They were recorded by a three-component flux-gate magnetometer LEMI-025 made at the Lviv Centre of the Institute for Space Research (<https://www.isr.lviv.ua/lemi025.htm>). The wave fluctuations were studied for three components of the magnetic field: X (northern) – the meridional component with the positive direction towards the North; Y (eastern) – the zonal component along the geographic parallel towards the East; Z – the vertical component directed vertically down. The magnetometer's resolution was no more than 0.1 nT. The data were sampled at one-second intervals, allowing us to study geomagnetic pulsations and wave disturbances with AGW periods.

Let us analyse the magnetometry data for January–March 2024. The geomagnetic conditions were mostly calm. According to <https://omniweb.gsfc.nasa.gov/form/dx1.html>, in January and February 2024, the $K_p \cdot 10$ index reached 40 only on some days (Fig. 1). In March, there were two geomagnetic storms: one on March 3 ($K_p \cdot 10$ peaked at 63) and the more powerful on March 24 (maximum $K_p \cdot 10$ of 83). We will show that the magnetic field regularly fluctuated with 5- to 60-min periods on calm days. On days of high geomagnetic activity, such wave disturbances were also seen, and their amplitudes were much larger.

Regardless of the wave's nature, an experimental study requires separating the wave fluctuations from large-scale changes in the measured parameters (trends). Magnetic field fluctuations were isolated using a moving average technique. The averaging window depended on the time scale to be selected from the initial data. Fluctuations of the field's components (δB_x , δB_y , and δB_z) were determined as the differences between the original sequences of data and the averaged ones. The coordinated course of fluctuations of various magnetic field components after trend removal allows for minimizing uncertainties in the data.

Finding the magnetic response to AGW propagation requires posing a set of criteria to select wave events for analysis. According to satellite data, AGW packets in the upper atmosphere last, on average, 3–5 periods (Innis & Conde, 2002; Fedorenko et al., 2015). Presumably, electromagnetic responses to AGW should be similar to the waves' signatures in a neutral atmosphere. Thus, a single wave event is defined here as a pronounced quasi-periodic packet lasting for more than two oscillation periods in the 5- to 60-minute range. Before applying the spectral analysis, each wave train was selected and examined visually to exclude possible abrupt changes of a non-wave nature.

Fragments of data treatment to separate wave events are shown in Figures 2 and 3; the example is based on the records of January 27, 2024 (UT evening). That afternoon, the geomagnetic activity was very low ($K_p \cdot 10 = 7$). The left column (Fig. 2) shows the three measured components of the magnetic field: besides trends, field fluctuations of various time scales can be seen. The right column shows the magnetic field's fluctuations after the moving average method was applied to every component: there is a wave packet at approximately 21UT–22.5UT in all cases. This packet's δB_x , δB_y , and δB_z are shown in Figure 3a. δB_x and δB_y remain in the syn-phase, and δB_z in the anti-phase to the two, although the packet itself is not monochromatic. Figure 3b shows the amplitude wavelet-spectrum for δB_x , drawn in Matlab using the complex Morlet wavelet: most

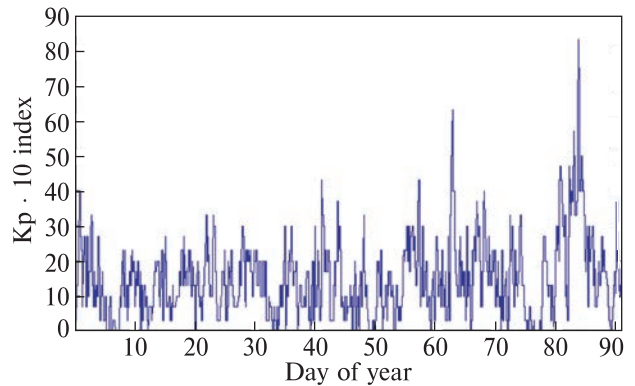


Figure 1. The value of $K_p \cdot 10$ index in January–March 2024, according to <https://omniweb.gsfc.nasa.gov/form/dx1.html>

fluctuations have a 10–12 min period with maximum amplitude around 22UT.

Note that here and further in the paper, the division of data into daily intervals refers to UT. That is, this division is conditional in terms of solar illumination at the Akademik Vernadsky station. The difference between UT and local solar time at the station is about 4 hours. During the study period (January–March), observations were carried out in sunlight for most of the day.

Often, when a magnetic field is measured, fluctuations of different time scales are superimposed. In this case, to separate various time scales, one should use moving average windows with different numbers of averaging points. Figure 4a provides a clear example of such superposition: it shows a sequence of δB_x records after applying a moving average window of 15 min. The amplitude wavelet spectrum in Figure 4b presents Pc4 geomagnetic pulsations with a period of ~ 1.5 min (noticeable in the lower part of the spectrum) overlaying quasi-sinusoidal fluctuations with a period of ~ 12 min. To obtain a more detailed picture of the spectrum for the short periods, we applied a window of 2 min to the original dataset. The resulting profile is typical for geomagnetic pulsations (Fig. 4c). Pc4 pulsations are the most common in geomagnetically calm conditions. They are observed in different latitudes. They can be recognized as series of long-term wave packets, indicating their resonance origin. According to

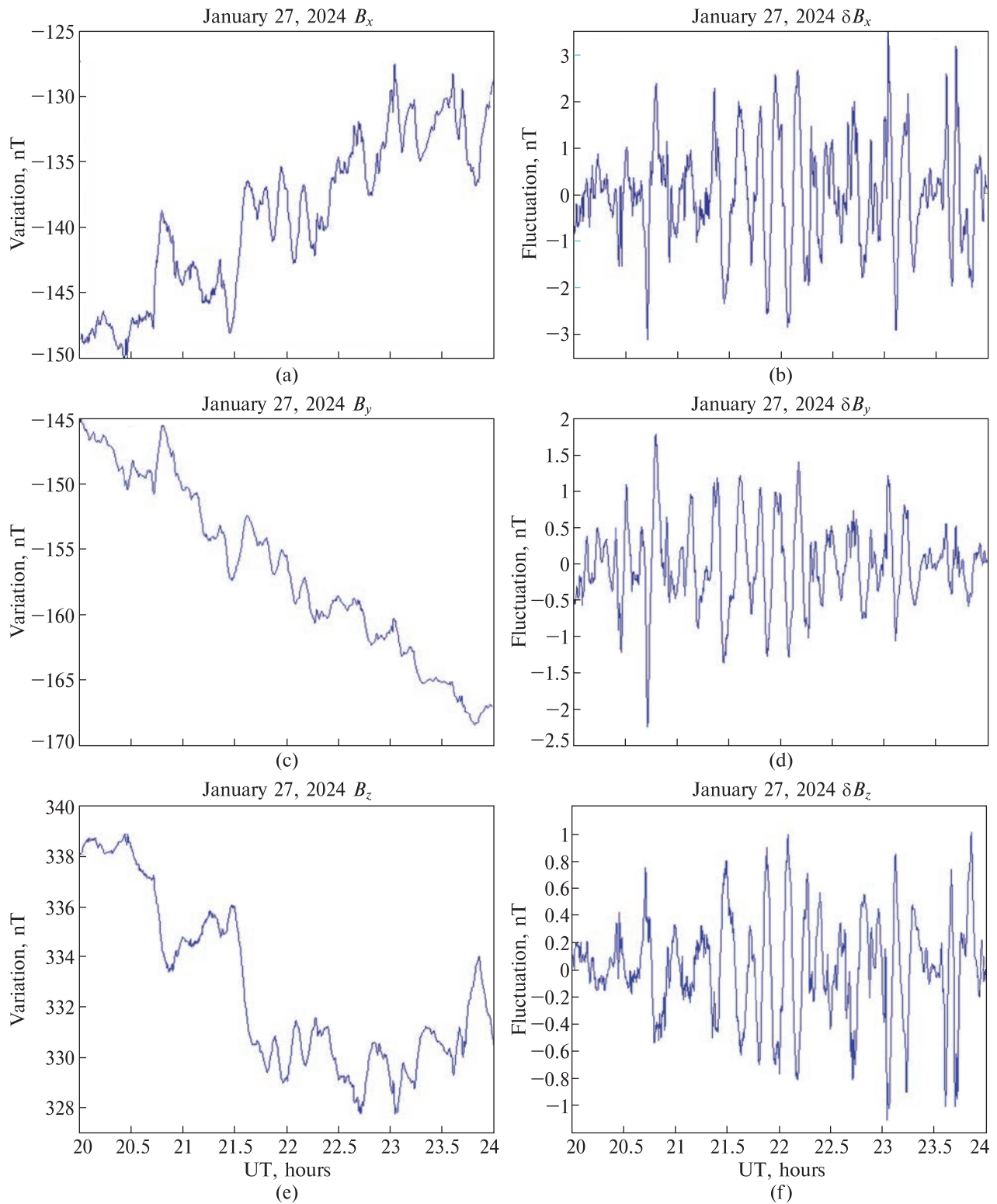


Figure 2. Variation of the components of the magnetic field on the evening (UT) of January 27, 2024, according to the records of the Akademik Vernadsky station (left) and the respective δB_x , δB_y , and δB_z fluctuations after the moving average filter (window of 30 min) was applied (right)

spectral analysis of the pulsations in Figure 4c, their period varies somewhat in the 1–1.5 min range (Fig. 4d).

We processed every day in January–March 2024 and studied magnetic field fluctuations in the 5–60 min range. The range is rather wide, as the minimum and maximum periods differ by an order of magnitude. That is why we started by applying a moving average window of 60 min. Afterward, we selected pronounced packets during the day and used wavelet analysis to identify the periods in the fluctuation ranges of δB_x , δB_y , and δB_z . Then, we used a smaller window of 10 min to isolate the lesser periods in the spectrum better. As the window size was reduced, wave harmonics of the larger periods remained in the spectrum, but their amplitudes became cut according to the filter’s frequency response.

Since the magnetometer’s resolution was no more than 0.1 nT, we selected fluctuations with amplitudes over ~ 1 nT in the δB_x and δB_y components. The corresponding minimum values of δB_z are usually less than ~ 0.3 – 0.5 nT. Notably, a large part of weak wave events with amplitudes < 1 nT in the δB_x and δB_y components remained outside the study’s scope.

3 Results

3.1 Amplitude analysis of magnetic field fluctuations

We analysed 500 wave packets: 165 in January, 137 in February, and 198 in March. On average, there were 4 to 6 wave events per day. The numbers of observed events in separate components are lower (358 events for δB_x , 378 for δB_y , and 388 for δB_z) as the fluctuations did not always occur in all three.

Figure 5 presents all wave events we studied in the three components of the field. The vertical axis shows the fluctuations’ amplitudes. The horizontal one shows the chronology of wave events every month. The left column (Fig. 5 a, c, e) compares the amplitudes of the δB_x and δB_y components, the right (Fig. 5 b, d, f), the amplitudes of δB_x and δB_z . The fluctuations did not always coincide in all field components. The amplitudes of δB_x and δB_y horizontal components are comparable and are, on average, a few nT in geomagnetically calm conditions. Amplitudes of the vertical component δB_z fluctuations are usually 2–3 times lesser than amplitudes of δB_x and δB_y .

There were two geomagnetic storms: on March 3 (maximum $K_p \cdot 10 = 63$) and March 24 (max-

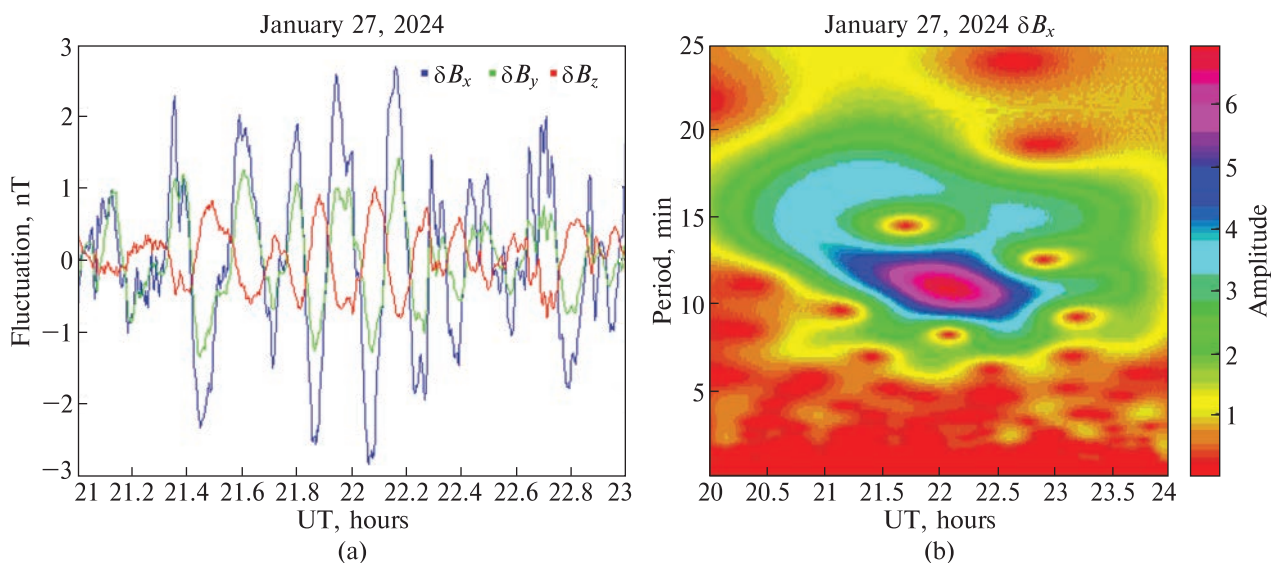


Figure 3. (a) Fluctuations of the δB_x , δB_y , and δB_z magnetic field components and (b) the relative amplitude of the wavelet spectrum for the horizontal δB_x fluctuation

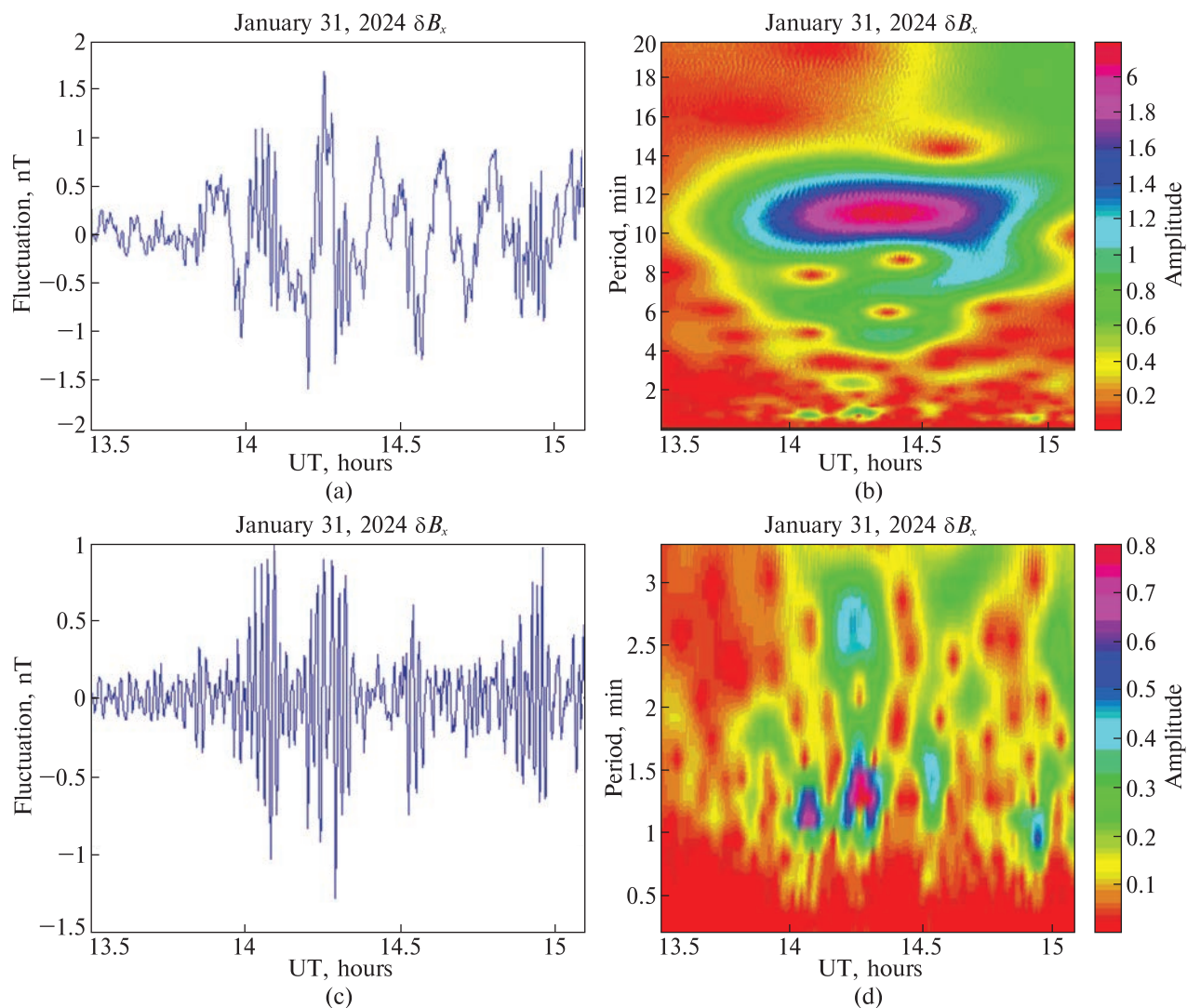


Figure 4. An example of superposition of geomagnetic fluctuations with AGW periods and Pc 4 geomagnetic pulsations. (a), (c) Magnetic field fluctuations after applying the moving average window of (a) 15 min or (c) 2 min (b), (d) The corresponding relative amplitude of the wavelet spectra

imum $K_p \cdot 10 = 83$). Two peaks can be seen in Figure 5 e, f (March), corresponding to the simultaneous growth of amplitudes of all components during storms. Each of the components δB_x and δB_y reached approximately 17 nT and 22 nT during these storms. Their maximum amplitudes during storms were approximately proportional to the maximum values of the K_p indexes. Changes in fluctuations' amplitudes during the magnetic storms require a separate study.

The observed ratios of fluctuation amplitudes for the horizontal and vertical components of the magnetic field show that the perturbation vector $\delta \vec{B} = (\delta B_x, \delta B_y, \delta B_z)$ is tilted close to the horizontal plane. Let us determine the angle φ between vector $\delta \vec{B}$ and the horizontal plane. The projection of $\delta \vec{B}$ onto the horizontal plane $\delta B_h = \delta B \cos \varphi$, where $\delta B_h = \sqrt{\delta B_x^2 + \delta B_y^2}$, and the vertical projection $\delta B_z = \delta B \sin \varphi$. Then, the angle φ is determined from the ratio $\operatorname{tg} \varphi = \delta B_z / \delta B_h$. The dynamics

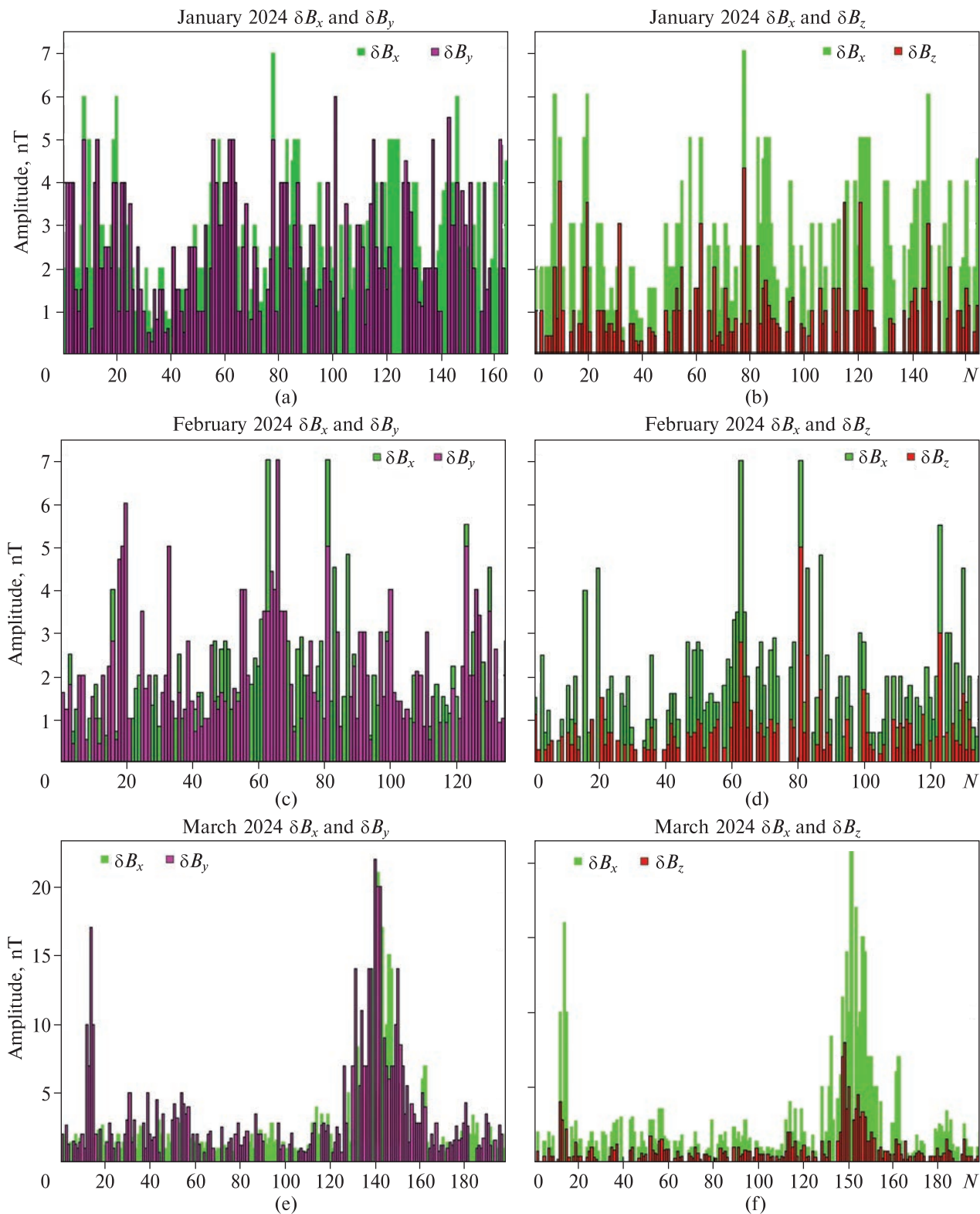


Figure 5. Amplitudes of the magnetic field fluctuation of horizontal δB_x and δB_y components (left) and horizontal δB_x and vertical δB_z components (right) for the studied wave events in January, February, and March 2024

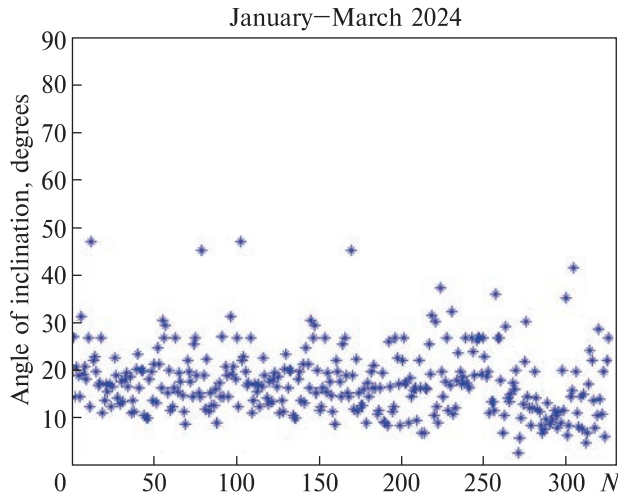


Figure 6. The angle of the fluctuation vector $\delta\vec{B}$ tilt to the horizontal plane for the studied wave events in January–March with $\delta B_z \neq 0$

of φ is given in Figure 6. The horizontal axis shows the number of wave events in January–March 2024. The value of φ mostly varied within 10° – 30° ; the three-month average is around 17.3° .

3.2 Diurnal variability of magnetic field fluctuations

Analysis of the wave events reveals such daily patterns:

- 1) if fluctuations occur simultaneously in all three components of the magnetic field, it mostly happens in the evening (UT);
- 2) at night, fluctuations are most frequent in the δB_x and δB_z components and rare in the δB_y ;
- 3) fluctuations in the δB_y component are mostly seen during the day; in other components, they are very weak or unnoticeable.

We then plotted the fluctuations separately for the three components depending on the hour for a more detailed analysis (Fig. 7 a, b, c). Every wave event was assigned the timestamp (UT) when the wave packet had the maximum amplitude, as determined by wavelet analysis. The daily distribution of the module of magnetic field fluctuations $\delta B = \sqrt{\delta B_x^2 + \delta B_y^2 + \delta B_z^2}$ is given in Figure 7d. There are three clear intervals during the day when the

wave events are registered most frequently. A comparison of the component-specific histograms in Figure 7 a, b, c shows that at 0–4UT, most events are of the $(\delta B_x, 0, \delta B_z)$ kind, while the $(\delta B_x, \delta B_y, \delta B_z)$ events are much fewer. At 10–14UT, most are $(0, \delta B_y, 0)$, and $(0, \delta B_y, \delta B_z)$ are fewer. In the evening (19–23UT), most wave events are $(\delta B_x, \delta B_y, \delta B_z)$, noticeable in all three components.

To summarize, in geomagnetically calm conditions, the wave activity in the meridional (B_x) and vertical (B_z) components is mostly registered in the morning and evening (UT). In the zonal component B_y , wave disturbances mostly happen from 10 to 14 hours UT. The patterns are evidence of the $\delta\vec{B}$ vector’s predominant direction changing depending on the UT.

The daily patterns of magnetic field fluctuations depend on the UT time. This probably indicates a decisive influence on the daily distribution of the auroral oval location relative to the station, which also depends on UT. The period (January–March) is not sufficient to study the influence of sunlight on magnetic fluctuations. To study this effect, we plan to use data throughout 2024.

3.3 Distribution of magnetic field fluctuations by periods

The distribution of wave events depending on the time of the day is plotted in Figure 8. Among all studied events, two groups of periods predominate. One is the fraction with periods shorter than 12 min, which borders the Brunt–Väisälä period of ~ 5 min (the minimum permissible period of AGW). The other demonstrates the maximum at 25–35 min. Two pronounced period groups can indicate different origins of the wave fluctuations. For example, AGW periods and Pc5 geomagnetic pulsations’ periods overlap in the 5–10 min range. However, Pc5 pulsations are observed in the area of the auroral oval during a substorm’s recovery phase. Long-periodic pulsations of the Pc6 type are observed in almost the same period range as the medium-scale AGWs.

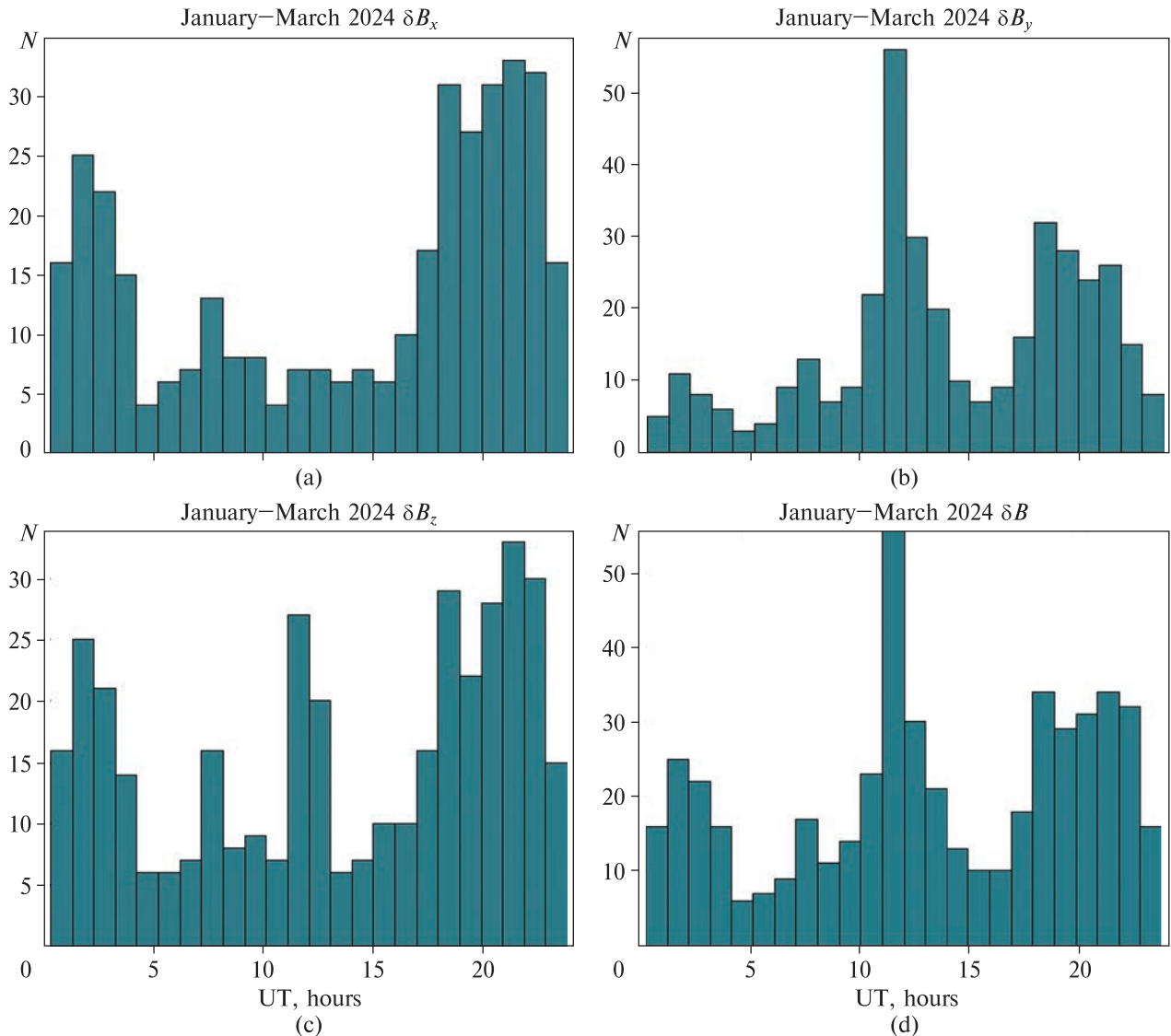


Figure 7. Distribution of the wave events (N) depending on the time of the day (UT) in three components of the magnetic field in January–March 2024: a) δB_x (358 events); b) δB_y (378); c) δB_z (388); d) δB (500)

However, the Ps6 pulsations are mostly seen only in the B_y component of the magnetic field and are also connected to substorms (Pulkkinen et al., 2003). Systematic registration of wave events in geomagnetically quiet conditions is probably evidence of their connection with AGWs which permanently exist in the atmosphere. Theory predicts a continuous spectrum of freely propagating AGWs in the atmosphere. Therefore, the two pronounced period groups can indicate AGWs of

different origins. Thus, periods around 30 min are more typical for freely propagating AGWs coming in from the sources below. Periods of 5–12 min can belong to AGWs generated by auroral sources directly at the heights of the E-region. A sharp altitudinal gradient of temperature at these heights favors their quasi-horizontal propagation. The predominance of wave events with small periods is evidence of a significant number of such AGWs at the heights of the polar dynamo-region.

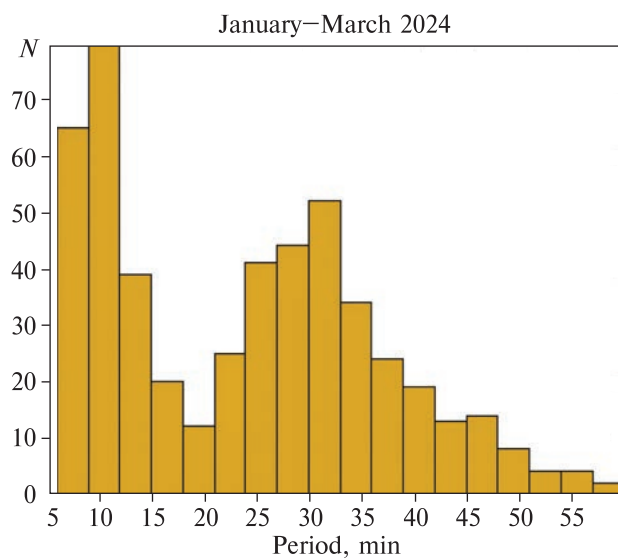


Figure 8. Distribution of wave events (N) over period size in January–March 2024

The observed two-period groups of the AGW magnetic response may be an important experimental manifestation of the separation of waves “from below” from those generated directly by auroral sources. Such a unique opportunity arises precisely in the polar regions where AGW from powerful auroral sources coexist with the waves from tropospheric and lithospheric sources. Akademik Vernadsky station is located in a very active meteorological region of the Earth. Therefore, the station records electromagnetic responses caused by AGW from tropospheric sources (Yampolsky et al., 2004). On the other hand, the Antarctic station is located at a fairly short distance from the auroral oval. Unlike influences “from below”, the conditions for recording influences “from above” should depend on geomagnetic activity and the moment of UT. The location of the oval relative to the observation station depends on UT. With the development of geomagnetic activity, the power of auroral sources increases, and the oval itself shifts to lower geomagnetic latitudes. This facilitates the observation of such waves at Akademik Vernadsky station. Therefore, it is important to investigate further the relationship between the two groups of peri-

ods of the AGW magnetic response during geomagnetic disturbances.

4 Discussion

We consider that the fluctuations of $\delta\vec{B}$, systematically observable in the 5- to 60-min period range in different geomagnetic conditions, mostly result from AGW propagation. These atmospheric waves can cause electromagnetic response at the height of the E-region of the ionosphere via two different pathways (Yampolsky et al., 2004): generation of dynamo current and modulation of the present background currents. Our research does not allow us to establish with certainty which of these two pathways dominates in the observed wave disturbances of the magnetic field at the Akademik Vernadsky station. We shall now explain the daily patterns in fluctuations of separate components of the magnetic field (Fig. 7). The changes in $\delta\vec{B}$ direction depending on the time of day will be considered in relation to the two pathways of the magnetic field’s response to AGW propagation.

Let us suppose that the effect is mostly caused by periodic modulation of background currents at the heights of the E-region of the ionosphere. The character of AGW modulation of the polar currents depends on their configuration. Under this scenario, the daily features of the magnetic response to AGW propagation in the δB_x and δB_y components can be caused by the system of currents changing over the day. The dependence of the fluctuations’ amplitudes on the Kp index is clearly seen for the two storms in March (Fig. 5 e, f), which is also evidence of background currents being modulated in the E-region. A significant enhancement in the polar current systems during geomagnetic distortions will cause an answering growth in the magnetic response to AGW. However, the tilt of force lines of the magnetic field at the station is around 58° , and the system of polar currents in geomagnetically calm conditions is mostly limited by the geomagnetic latitudes of the auroral oval. Thus, the effect of cur-

rents' modulation is probably not the main influence governing the magnetic fluctuations in the area. However, its relative contribution can grow under high geomagnetic activity.

The electromagnetic effect of dynamo-current generation by AGWs can be significant since large-amplitude AGWs are permanently present in the polar areas (Innis & Conde, 2002; Fedorenko et al., 2015). In this case, the observed daily patterns of the fluctuations in different components of the magnetic field may be related to the prevailing azimuths of AGW propagation. Thus, measurements taken by the Dynamics Explorer 2 satellite established that large-amplitude AGWs systematically propagate against the wind in the polar thermosphere of both hemispheres (Fedorenko et al., 2024). Polar AGWs can reach even low geomagnetic latitudes over the Antarctic in December–February and over the Arctic in June–August (Vlasov et al., 2022). Presumably, at the heights of the E-region in the ionosphere, the predominant azimuths of AGW propagation also change depending on the time of day following the daily restructuring of the winds over the station. If AGWs propagate mostly along the meridian, geomagnetic field fluctuations will be the most pronounced in the zonal component δB_y . If, on the other hand, AGWs spread along the parallel, the magnetic fluctuations will be the most pronounced in the δB_x component. Then, the identified azimuths of AGW propagation changing over the day also explain the daily patterns in the fluctuations of different magnetic field components.

AGWs are considered as important transport agents that redistribute the energy of various disturbances in the atmosphere. The discovery of two separate period groups of AGW magnetic response indicates that AGWs effectively implement influences from above and below. The possibility of experimentally separating these influences is of great importance for understanding the energy interaction between different altitude levels of the atmosphere. However, our three-month research is insufficient to determine the global features of the magnetic response of the AGW, particularly

seasonal patterns. In the future, we plan to expand similar studies based on magnetometric data at the Akademik Vernadsky station throughout 2024. Further statistical research (such as establishing the seasonal patterns of wave fluctuations over the whole year) will allow us to understand better the contribution of each considered pathway to the electromagnetic response to AGW propagation. Special attention will be paid to the AGW magnetic response during geomagnetic storms. Of particular interest is how the contribution of short-period disturbances (5–12 min) changes with increasing geomagnetic activity.

5 Conclusions

Our work mainly aimed to study the magnetic response to AGW propagation in the polar areas. We analysed wave fluctuations of the magnetic field in the period range of 5 to 60 min based on three-component magnetometric measurements at the Akademik Vernadsky station. These periods correspond to the middle-scale AGW propagating through the atmosphere. We registered and analysed 500 wave events in January–March 2024. Every event was a pronounced wave packet consisting of several fluctuation periods. Generally, the fluctuations' amplitudes were several times larger in the horizontal δB_x (meridional) and δB_y (zonal) components than in the vertical component δB_z . These amplitudes were ~one nT to several nTs in geomagnetically calm conditions and reached dozens of nTs during the two geomagnetic storms in March. Given the ratios of the amplitudes in the fluctuations of the horizontal and vertical components, the tilt of the perturbation vector $\delta \vec{B}$ to the horizontal plane was determined.

We plotted the distribution of the frequencies of fluctuations' occurrence depending on the hour of the day. There were distinct daily patterns for different components of the magnetic field. In the magnetically calm conditions, the meridional component δB_x fluctuated mostly in the morning and in the evening. In the middle of the day, they

were the least pronounced. On the other hand, the wave disturbances in the zonal component δB_y are mostly registered in the middle of the day and in the evening hours. The daily pattern of the fluctuations in the vertical δB_z component mostly coincides with that of the δB_x component.

In January and February, the geomagnetic situation was relatively calm, a good setting for diagnosing wave processes unrelated to the geomagnetic activity. In March, there were two geomagnetic storms. As the storm grew, a sharp increase in the amplitudes of magnetic field fluctuations was observed. For the magnetic fluctuations with AGW periods, the amplitudes grew proportionally to the Kp index. In our opinion, a great enhancement in the system of polar currents during the geomagnetic disturbances leads to a corresponding increase in the magnetic response to AGW.

Two main groups of periods were seen in the distributions of wave fluctuations' periods during the three studied months. A large part of the observed fluctuations had periods of 5–12 min. The plot also showed another maximum (25–30 min). These two groups of periods can indicate AGWs of different origins. AGWs generated directly by the auroral sources at the E-region heights can have periods of 5–12 min. A sharp altitudinal gradient of temperature contributes to their quasi-horizontal propagation at these heights. The 25–30 min periods, on the other hand, are more typical for the freely propagating AGW coming in from the sources below.

The division of the periods of the AGW electromagnetic response into two separate groups may be experimental evidence of the coexistence of influences “from above” and “from below” at ionospheric altitudes. It is important to establish which mechanism prevails in the polar ionosphere under geomagnetically quiet or disturbed conditions, depending on the time of day or season. This will improve the understanding of the interaction between space and surface weather systems.

Author contributions. Investigation and preparation of the article, A.F.; investigation and inter-

pretation, E.K. and A.V.; data processing and editing, I.Z.

Funding. This work was supported by the State Institution National Antarctic Scientific Center of the Ministry of Education and Science of Ukraine within the framework of the State Special-Purpose Research Program in Antarctica for 2011–2025. The authors also thank the Center for providing magnetometer data of the Akademik Vernadsky station.

Conflict of Interest. The authors declare no conflict of interest.

References

- Fedorenko, A. K., Bespalova, A. V., Cheremnykh, O. K., & Kryuchkov, E. I. (2015). A dominant acoustic-gravity mode in the polar thermosphere. *Annales Geophysicae*, 33(1), 101–108. <https://doi.org/10.5194/angeo-33-101-2015>
- Fedorenko, A. K., Kryuchkov, E. I., Cheremnykh, O. K., & Melnychuk, S. V. (2024). Propagation of acoustic-gravity waves in inhomogeneous wind flows of the polar atmosphere. *Kinematics and Physics of Celestial Bodies*, 40, 15–23. <https://doi.org/10.3103/S0884591324010045>
- Heyns, M. J., Lotz, S. I., & Gaunt, C. T. (2020). Geomagnetic pulsations driving geomagnetically induced currents. *Space Weather*, 19(2), e2020SW002557. <https://doi.org/10.1029/2020SW002557>
- Innis, J. L., & Conde, M. (2002). Characterization of acoustic-gravity waves in the upper thermosphere using Dynamics Explorer 2 Wind and Temperature Spectrometer (WATS) and Neutral Atmosphere Composition Spectrometer (NACS) data. *Journal of Geophysical Research: Space Physics*, 107(A12), SIA 1-1–SIA 1-22. <https://doi.org/10.1029/2002JA009370>
- Jacobson, A. R., & Bernhardt, P. A. (1985). Electrostatic effects in the coupling of upper atmospheric waves to ionospheric plasma. *Journal of Geophysical Research: Space Physics*, 90(A7), 6533–6541. <https://doi.org/10.1029/JA090iA07p06533>
- Kelley, M. C. (1989). *The Earth's Ionosphere. Plasma Physics and Electrodynamics*. Academic Press, Inc. <https://doi.org/10.1016/B978-0-12-404013-7.X5001-1>
- Lizunov, G., Skorokhod, T., Hayakawa, M., & Korepanov, V. (2020). Formation of ionospheric precursors of earthquakes – Probable mechanism and its substantiation. *Open Journal of Earthquake Research*, 9(2), 142–169. <https://doi.org/10.4236/ojer.2020.92009>
- McPherron, R. L. (2005). Magnetic pulsations: Their sources and relation to solar wind and geomagnetic activity. *Surveys in Geophysics*, 26, 545–592. <https://doi.org/10.1007/s10712-005-1758-7>

Negale, M. R., Taylor, M. J., Nicolls, M. J., Vadas, S. L., Nielsen, K., & Heinselman, C. J. (2018). Seasonal propagation characteristics of MSTIDs observed at high latitudes over Central Alaska using the Poker Flat Incoherent Scatter Radar. *Journal of Geophysical Research: Space Physics*, 123(7), 5717–5737. <https://doi.org/10.1029/2017JA024876>

Paznukhov, V. V., Sopin, A. A., Galushko, V. G., Kashcheyev, A. S., Koloskov, A. V., Yampolski, Y. M., & Zalizovski, A. V. (2022). Occurrence and characteristics of Traveling Ionospheric Disturbances in the Antarctic Peninsula region. *Journal of Geophysical Research: Space Physics*, 127(11), e2022JA030895. <https://doi.org/10.1029/2022JA030895>

Prakash, S., & Pandey, R. (1985). Generation of electric fields due to the gravity wave winds and their transmission to other ionospheric regions. *Journal of Atmospheric and Terrestrial Physics*, 47(4), 363–374. [https://doi.org/10.1016/0021-9169\(85\)90016-9](https://doi.org/10.1016/0021-9169(85)90016-9)

Pulkkinen, A., Thomson, A., Clarke, E., & McKay, A. (2003). April 2000 geomagnetic storm: Ionospheric drivers of large geomagnetically induced currents. *Annales Geophysicae*, 21(3), 709–717. <https://doi.org/10.5194/angeo-21-709-2003>

Saito, T. (1978). Long-period irregular magnetic pulsation, Pi3. *Space Science Reviews*, 21(4), 427–467. <https://doi.org/10.1007/BF00173068>

Vlasov, D. I., Fedorenko, A. K., Kryuchkov, E. I., Cheremnykh, O. K., & Zhuk, I. T. (2022). Seasonal features of the spatial distribution of atmospheric gravity waves in the Earth's polar thermosphere. *Kinematics and Physics of Celestial Bodies*, 38, 73–82. <https://doi.org/10.3103/s0884591322020076>

Yampolsky, Yu., Zalizovsky, A., Litvinenko, L., Lizunov, G., Groves, K., & Moldvin, M. (2004). Magnetic field variations in Antarctica and the conjugate region (New England) stimulated by cyclone activity. *Radio-Physics and Radio-Astronomy*, 9(2), 130–151.

Zhang, S.-R., Erickson, P. J., Coster, A. J., Rideout, W., Vierinen, J., Jonah, O., & Goncharenko, L. P. (2019). Subauroral and polar traveling ionospheric disturbances during the 7–9 September 2017 storms. *Space Weather*, 17(12), 1748–1764. <https://doi.org/10.1029/2019sw002325>

Received: 11 December 2024

Accepted: 11 January 2025

Алла Федоренко*, Євген Крючков,
Анна Войцеховська, Ігор Жук

Інститут космічних досліджень Національної академії наук України
та Державного космічного агентства України, м. Київ, 03187, Україна

* Автор для кореспонденції: fedorenkoak@gmail.com

Дослідження магнітного відгуку на поширення АГХ за вимірами на станції «Академік Вернадський»

Реферат. З метою пошуку електромагнітного відгуку на поширення атмосферних гравітаційних хвиль (АГХ) досліджено хвильові флуктуації магнітного поля за даними вимірювань на Українській антарктичній станції «Академік Вернадський». Проаналізовано неперервні дані вимірювань трьох компонент геомагнітного поля впродовж січня-березня 2024 року. Розглянуто хвильові флуктуації магнітного поля в діапазоні періодів 5–60 хв, що відповідають середньомасштабним АГХ в атмосфері Землі. Впродовж січня-березня всього було проаналізовано 500 хвильових подій, амплітуди яких склали від ~1 нТл до кількох десятків нТл. Спостерігалось дві групи переважаючих періодів: ~5–12 хв (включаючи період Брента-Вяйсяля) та 25–30 хв. Висловлено припущення, що існування цих двох груп періодів вказує на різне походження АГХ. Цей отриманий новий результат показує на експериментальну можливість відокремлення ефектів впливів АГХ «знизу» та «згори». Визначено часові інтервали впродовж доби, коли флуктуації магнітного поля спостерігаються найчастіше. Одночасно у всіх трьох компонентах магнітного поля флуктуації спостерігаються у вечірні години. У геомагнітно-спокійних умовах помічено добову асиметрію у частоті появи меридіональних і зональних збурень. Хвильова активність у меридіональній B_x та вертикальній B_z компонентах магнітного поля реєструється переважно вранці та увечері за UT. У зональній компоненті B_y хвильові збурення переважають вдень від 10 до 14 годин UT, а також спостерігаються увечері. У березні 2024 року сталися дві геомагнітні бурі, під час яких спостерігалось одночасне зростання амплітуд флуктуацій магнітного поля у різних діапазонах періодів. Досліджені флуктуації магнітного поля можуть бути спричинені модуляцією полярних струмових систем та (або) генерацією динамо-струму при поширенні АГХ на висотах Е-області іоносфери. Для того щоб встановити, який механізм переважає у формуванні спостережуваного електромагнітного відгуку, необхідні подальші дослідження.

Ключові слова: атмосферні гравітаційні хвилі, геомагнітні пульсації, флуктуації магнітного поля